

Ge_xSi_{1-x} strained-layer superlattice waveguide photodetectors operating near 1.3 μm

H. Temkin, T. P. Pearsall, J. C. Bean, R. A. Logan, and S. Luryi
 AT&T Bell Laboratories, Murray Hill, New Jersey 07974

(Received 21 November 1985; accepted for publication 18 February 1986)

Properties of Ge_xSi_{1-x} strained-layer *p-i-n* detectors, in which the strained-layer superlattice itself was used as an absorption region, have been studied for the first time. These devices were grown on (100)Si by molecular beam epitaxy. Using waveguide geometry we have obtained internal quantum efficiencies on the order of 40% at 1.3 μm in superlattices with the Ge fraction $x = 0.6$. The superlattice detectors show the frequency response bandwidth of over 1 GHz and uniformly excellent electrical characteristics for values of x as large as 0.8.

Recent advances in Si molecular beam epitaxy¹⁻³ have opened the possibility of extending the spectral response of Si photodetectors into the 1.3-μm spectral region through the use of heterostructures composed of Ge and Si. Such detectors, combining the best features of Si and Ge devices, would be of interest in a variety of fiber-optic and other applications.

The performance of near infrared devices prepared on Si substrates has recently been discussed by Luryi *et al.*⁴ and Kastalsky *et al.*⁵ These photodetectors incorporated ~1-μm-thick Ge layers grown on either *p*- or *n*-type Si substrates. Two different routes were taken in order to avoid deleterious effects of the large (4%) lattice mismatch between Si and Ge. First⁴ the active detector structure (Ge layer) was separated from the substrate-epitaxial layer interface by a graded SiGe layer. This approach produced photodiodes with a high quantum efficiency of 40% at the wavelength of 1.45 μm. However, the graded layer did not stop threading dislocations from reaching into the active layer, resulting in high leakage and low reverse breakdown voltage of ~3 V. In the second approach⁵ the graded layer was replaced by a Ge_xSi_{1-x}/Si strained-layer superlattice (SLS). These have been grown with a very high degree of structural perfection⁶ and proved to be very effective dislocation barriers. Indeed, leakage currents were reduced by an order of magnitude in devices incorporating SLS barriers. However, these devices have not yet achieved high quantum efficiencies.

In this work we demonstrate a radically different diode configuration in which the Ge_xSi_{1-x} SLS itself is used as an absorbing region. In order to provide efficient photoreponse in the 1.3-μm region, the Ge fraction in the Ge_xSi_{1-x} layers of these superlattices must be on the order of 0.4-0.6. However, in a coherent SLS of this composition, the thick-

ness of a Ge-rich layer is limited to less than 100 Å.⁶ In order to provide a sufficiently large absorption depth the incident light is launched into the buried waveguide formed by the larger index of refraction of the superlattice layer sandwiched between layers of Si. A detailed model of the optimum waveguide parameters will be described elsewhere.⁷ The waveguide photodetectors are wavelength selective, exhibit excellent *I-V* characteristics, and internal quantum efficiency of the order of 40% at 1.3 μm. Their modulation bandwidth exceeds 1 GHz.

A schematic diagram of the device structure is shown in Fig. 1. Epitaxial layers were grown on (100) oriented *n*-type Si wafers. The photodiode consists of an *n*-Si buffer layer followed by the *n*-doped superlattice absorption layer. The thickness of the Ge_xSi_{1-x} layer was adjusted for each Ge concentration in order to retain the commensurate growth of the SLS structure.⁶ The example shown in Fig. 1 is made of 20 wells of Ge_{0.6}Si_{0.4}, each 60 Å thick, separated by 290-Å-thick Si barriers. With the Ge fraction increased to 0.80 the well thickness had to be reduced to less than 20 Å. With the Ge fraction increasing from $x = 0.25$ to 0.80 the number of layers was kept constant and the thickness of wells and barriers adjusted to yield the active layer (waveguide) thickness of 6500 Å. The nonintentionally doped (*i*) superlattice region was capped with a 1-μm-thick *p*-Si layer doped by coimplantation with boron to ~5 × 10¹⁶ cm⁻³ followed by a thin *p*-Si (1 × 10¹⁷ cm⁻³) contact layer.

The reverse-biased current-voltage characteristics of the 300-μm-long and 60-μm-wide CF₄ etched mesa diode are shown in Fig. 2. The Ge fraction in the active layer superlattice is equal to $x = 0.6$. No attempts were made to either passivate or bury the exposed side walls. After thinning the wafer to approximately 100 μm the front facet was fabricated by cleaving. Despite this simple processing procedure,

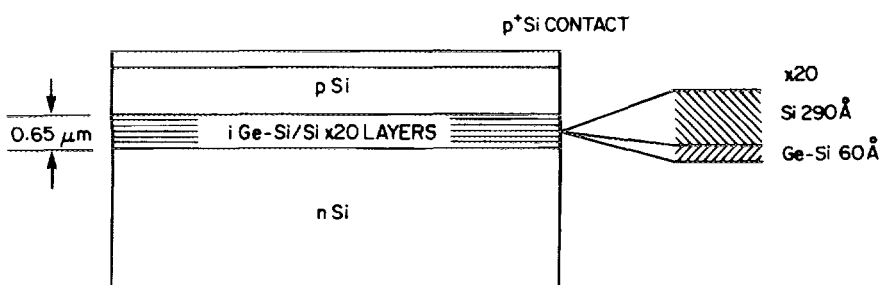


FIG. 1. Schematic diagram of the device structure.

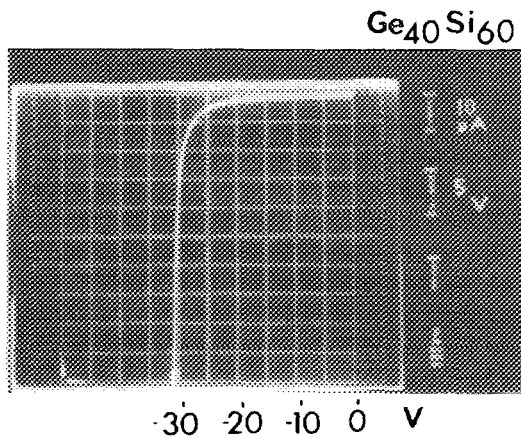


FIG. 2. Dark current-voltage characteristics of a 300- μm -long waveguide. The active superlattice consists of 20 layers of $\text{Ge}_{0.4}\text{Si}_{0.6}$, each 60 \AA wide.

the electrical characteristics of the SLS p - i - n 's are uniformly excellent. Reverse breakdown voltages of all the devices grown under conditions of commensurate epitaxy vary from 30 to 38 V, irrespective of the Ge fraction in the superlattice. The electrical characteristics are extremely uniform over any given wafer. This range of the breakdown voltages is consistent with the Si doping level⁸ and suggestive of the p - n junction within the top Si layer, an assumption supported by the absence of any dependence on the composition of the SLS. However, the leakage current increases slowly with the Ge fraction. At a reverse bias of -10 V, the leakage current changes from $\sim 0.4 \mu\text{A}$ (or $9.5 \times 10^{-4} \text{ A/cm}^2$) for $x = 0.4$ to as much as $3 \mu\text{A}$ (or $7.1 \times 10^{-3} \text{ A/cm}^2$) for $x = 0.6$ to 0.8. This increase is nearly linear in x and seems too small to be accounted for by the SLS band-gap changes. Variation in the size of the photodiodes shows the leakage current changing as the diode surface area, suggesting a connection with structural imperfections. While the preliminary results of the defect etching experiments indicate a constant dislocation etch pit density of $(1-2) \times 10^4 \text{ cm}^{-2}$ the diameter of etch pits increases dramatically, by up to a factor of 10, with increasing x . The possible formation of dislocation clusters will be examined by transmission electron microscopy.

The breakdown voltages and the leakage currents of the SLS diodes are comparable to state-of-the-art Ge avalanche photodiodes.⁹ In those very sophisticated, buried junction devices, reverse breakdown voltages of 32 V and leakage current densities of $1 \times 10^{-3} \text{ A/cm}^2$ at 10 V have been obtained.

Little is known, at present, about the optical properties of coherently strained $\text{Ge}_x\text{Si}_{1-x}$ alloys. It has been recently pointed out by People¹⁰ that the lattice mismatch strain should result in a significant reduction of the indirect band gap. Recent photocurrent experiments of Lang *et al.*¹¹ have confirmed this possibility. Figure 3 shows the first spectral response measurements of $\text{Ge}_x\text{Si}_{1-x}$ SLS waveguides as a function of Ge fraction x . These experiments were performed at room temperature using a tungsten lamp excitation and conventional lock-in detection. Absolute values of the internal quantum efficiency ($\pm 20\%$) were obtained using calibrated InGaAsP waveguide detectors. The curves shown in Fig. 3 are for unpolarized light. Excitonic polariza-

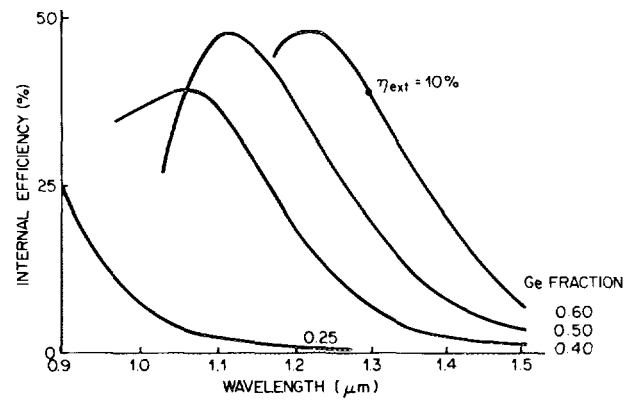


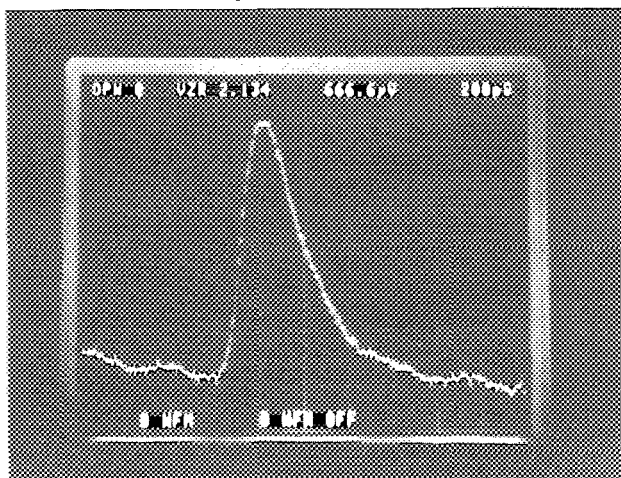
FIG. 3. Room-temperature spectral response of the superlattice p - i - n as a function of Ge content of the active layer. Spectral response measurements were carried out at zero bias in 4-mm-long devices.

tion effects expected in quantum well superlattices were not observed. Similarly, no spectral shifts were observed at reverse bias voltages of up to -10 V, corresponding to an applied field of $1.6 \times 10^5 \text{ V/cm}$. The long wavelength photocurrent response of the SLS waveguides increases sharply with increased Ge content of the active layer. For $x = 0.25$ only very weak response is observed at wavelengths longer than $0.95 \mu\text{m}$. A dramatic change occurs for waveguides with $x > 0.40$ which clearly show efficient response at wavelengths as long as $1.3 \mu\text{m}$. As the Ge fraction is increased from $x = 0.40$ in 10% increments the photocurrent response peaks at 1.08, 1.12, and $1.23 \mu\text{m}$, respectively. The peak internal quantum efficiency is conservatively estimated at 47%. The high efficiency is made possible by the long absorption length inherent in the waveguide configuration. Despite this structural enhancement, the photocurrent response at $1.5 \mu\text{m}$ is very low and only marginal improvements are expected for higher x where the very thin layers required will result in a competing quantum well shift.

The decrease in efficiency at shorter wavelengths, closer to the Si band edge, is attributed to the reduction in the effective dielectric constant of the waveguide. The maximum photocurrent response is at a considerably shorter wavelength than the SLS band gap as determined on the same samples by Lang and co-workers.¹¹ For instance, for $x = 0.5$ the indirect band gap lies at $1.50 \mu\text{m}$ (0.82 eV) at room temperature while the peak waveguide response occurs at $1.12 \mu\text{m}$ (1.10 eV). The waveguide photodiodes can operate as much as ~ 0.3 eV above the SLS band gap with the corresponding exponential enhancement of the absorption coefficient and quantum efficiency.

While the internal quantum efficiency indicates the maximum possible detector response, the external efficiency is a more immediate indicator of the device quality. In a wavelength geometry the external efficiency depends very strongly on the coupling conditions. Using a single-mode fiber butt coupled to the waveguide facet, quantum efficiency of 10.2% has been measured at $1.3 \mu\text{m}$. The external efficiency depends strongly on the bias voltage. It increases from less than 1% at zero bias to about 6% at 5 V and reaches its maximum value near 10 V. No further increase is observed at higher bias levels. This bias dependence of effi-

GeSi SLS pin



$$t_{\text{FWHM}} = 312 \text{ ps}$$

FIG. 4. Impulse response of a $\text{Ge}_{0.6}\text{Si}_{0.4}$ p - i - n detector illuminated with a 50-ps-long pulse of a mode-locked $1.3\text{-}\mu\text{m}$ laser. Device biased to $1/3$ of the breakdown voltage.

ciency is suggestive of carrier trapping at low applied field.

In view of the possible carrier trapping limitation on the frequency bandwidth of the SLS detectors, we have investigated their impulse response. Figure 4 shows the pulse response of $\text{Ge}_{0.6}\text{Si}_{0.4}$ detector illuminated by 50-ps-long pulses obtained from a mode-locked $1.3\text{-}\mu\text{m}$ laser. The pulse repetition rate was 720 MHz. The diode response time (full width at half-maximum) decreases from 500 ps at zero bias to $\sim 290\text{--}310$ ps at 10 V, or $1/3$ of the breakdown voltage. The speed is limited by the RC constant of the diode and not by any carrier trapping effects. This impulse response is equivalent to a 3-dB bandwidth on the order of 1 GHz. Similar bandwidth values have been obtained for Ge p - i - n detectors.⁹

The relatively low external efficiency is due to the dimensional mismatch between the 5 to $8\text{-}\mu\text{m}$ -diam optical fiber and $0.6\text{-}\mu\text{m}$ thickness of the active layer. The coupling

loss could be minimized by increasing the thickness of the $\text{Ge}_x\text{Si}_{1-x}$ SLS. High quality superlattices, free of misfit dislocations, have been grown with as much as 100 layers. Factors of 2–3 improvement could be realized by coupling light through a small lens placed at the fiber end, an approach routinely used in coupling laser light to single mode fibers. An even more attractive possibility is the SLS avalanche photodiode. The excellent electrical properties of our p - i - n devices indicate feasibility of reaching the field levels necessary for impact ionization. Since the junction and the avalanche region could be placed in the Si layers, gain similar to that obtainable in bulk Si devices, i.e., greater than a factor of 10, may be possible. These possibilities will be addressed in more detail by Luryi *et al.*⁷

We would like to thank V. Narayanamurti without whose enthusiastic support this work would not have been done. Many conversations with D. V. Lang and R. People were very stimulating and fruitful. We would also like to thank R. T. Lynch and A. Savage for excellent technical help.

¹J. C. Bean, L. C. Feldman, A. T. Fiory, S. Nakahara, and I. K. Robinson, *J. Vac. Sci. Technol. A* **2**, 436 (1984).

²J. C. Bean, in *Symposium in Layered Structures Epitaxy and Interfaces*, edited by J. M. Gibson and L. R. Dawson (Material Research Society, Pittsburgh, PA, 1985), p. 245.

³R. People, J. C. Bean, D. V. Lang, A. M. Sergent, H. L. Stormer, K. W. Wecht, R. T. Lynch, and K. Baldwin, *Appl. Phys. Lett.* **45**, 1231 (1984).

⁴S. Luryi, A. Kastalsky, and J. C. Bean, *IEEE Trans. Electron Devices* **ED-31**, 1135 (1984).

⁵A. Kastalsky, S. Luryi, J. C. Bean, and T. T. Sheng, in *Proceedings of the 1st International Symposium on Si Molecular Beam Epitaxy*, edited by J. C. Bean (Electrochemical Society, Pennington, NJ, 1985), p. 408.

⁶J. C. Bean, in *Proceedings of the 1st International Symposium on Si Molecular Beam Epitaxy*, edited by J. C. Bean (Electrochemical Society, Pennington, NJ, 1985), p. 339.

⁷S. Luryi, T. P. Pearsall, H. Temkin, and J. C. Bean (unpublished).

⁸S. M. Sze, *Physics of Semiconductor Devices* (Wiley-Interscience, New York, 1969), p. 115.

⁹S. Kagawa, T. Mikawa, and T. Kaneda, *Fujitsu Sci. Tech. J.* **18**, 397 (1982).

¹⁰R. People, *Phys. Rev. B* **32**, 405 (1985).

¹¹D. V. Lang, R. People, J. C. Bean, and A. M. Sergent, *Appl. Phys. Lett.* **47**, 1333 (1985).